IMAV2017-12
http://www.imavs.org/pdf/imav.2017.12

Robust Attitude Control for Quadrotors with External Disturbances

H. Nemati,* A. Naghash, S. Mozafari, and A. Jamei
Amirkabir University of Technology (Tehran Polytechnic), 424 Hafez Ave., Tehran 15875-4413, Iran

ABSTRACT

This study investigates a design procedure for a robust nonlinear control algorithm based on sliding mode control (SMC) to stabilize the attitude of a 3-DOF quadrotor UAV subject to external disturbances. Since traditional sliding mode controllers are sensitive against external disturbances in the reaching phase, a new algorithm is proposed to enhance the robust performance of an SMC strategy. Dynamic equations are obtained using Newton-Euler formalism and the quadrotor's centre of mass is assumed not to be coincident at the origin of body frame. The robust stability and the robust tracking property are achieved using the Lyapunov's direct method. Experimental results are given to highlight the effectiveness of the designed control strategy.

1 INTRODUCTION

Flight control of Unmanned Aerial Vehicles (UAVs) have received considerable attention from researchers recently because of numerous applications ranging from transportation (such as Amazon delivery system), security, rescue mission, agriculture, construction, traffic surveillance, image processing over nuclear reactors, management of natural risks, environment exploration, mapping, aerial cinematography, border prohibition and military. To accomplish these features which are executed in hazardous and inaccessible situations, the designed controller must be robust against environmental disturbances (such as wind gust) and parameter uncertainty (such as inertia variation).

Real systems exhibit hard nonlinearities such as Coulomb friction, actuator saturation, valve dead zones, gear backlash and hysteresis which may possess some discontinuous features that do not lend themselves to the linear approximation [1]. Nonlinear control systems provide a level of dynamic capabilities when dealing with parameter variations and unmodeled dynamics that linear approaches cannot deal with. Indeed, the success of a UAV mission strongly depends upon the precision of its attitude control in spite of the presence of environmental disturbances and large parameter uncertainties. Hence, the designed controller must be somewhat immune to variations across parameters in the model and be able to overcome the above inaccuracies. Sliding mode control (SMC) has been recognized as a robust control technique for quadrotor's attitude motion because of its inherent advantages of strong stability, disturbance rejection and low sensitivity to plant parameter variations [2].

The quadrotor is a four-propeller Vertical Take-Off and Landing (VTOL) rotorcraft which has been proven to be one of the efficient vehicles to achieve rapid turns and strong maneuverability compared to traditional aircraft. Over several years much research has been devoted to design of the attitude controller for the quadrotor UAV. In [3], a robust flight controller for a 6-DOF quadrotor model has been designed based on the sliding mode control driven by sliding mode disturbance observer (SMC-SMDO). This controller has been relied on the knowledge of the limits of the disturbance. Since the determination of the coefficients used in the sliding surface is difficult in practice, Hurwitz stability analysis has been employed in [4, 5] to obtain the nonlinear coefficients of the second order sliding manifold. Besides, the nonlinear sliding surface has been simplified by linearizing around the desired equilibrium points and then the nonlinear coefficients were calculated by Hurwitz stability. A super twisting sliding mode controller has been designed in [6] by utilizing a cascaded inner-outer loop structure for a quadrotor. Its robustness has been also compared against a traditional SMC, a popular linear controller (LQR-PD) and a nonlinear feedback linearization based controller subject to wind turbulence conditions and modeling uncertainties. Active disturbance rejection control are often used to eliminate the effect of the state coupling and uncertainties. The robust trajectory tracking problem of an autonomous quadrotor with obstacle avoidance based on the active disturbance rejection control has been introduced in [7]. The problem of attitude regulation for a quadrotor with parametric uncertainties and external disturbances has been studied theoretically by employing a novel adaptive fuzzy gain-scheduling sliding mode control approach in [8].

So far, a large number of references have been devoted to the theoretical analysis of a quadrotor flight controller based upon the linear and nonlinear control methods. There is much research for position/attitude control of a quadrotor in a real time. Model based controller for position and attitude trajectory tracking of a quadrotor have been introduced experimentally in [9]. The problem of designing and experimentally validating a controller based on a backstepping procedure for steering a quadrotor system along a trajectory subject to ex-

*Email address: hr.nemati@gmail.com

ternal disturbances has been addressed in [10, 11]. A high-performance flight control approach utilizing an active disturbance rejection technique for the quadrotors has been studied in [12]. Recently, second order sliding mode controllers which are the simplest class of the higer order sliding mode (HOSM) approach are taken into account experimentally by many researchers. A popular type of the second order sliding mode control, super twisting algorithm, has been utilized in [13] to stabilize a quadrotor UAV experimentally. However, HOSM is not able to ensure the finite time stability [14] and the system trajectory in the second order sliding mode control strategy is very slow when states are far away from the origin [15]. Traditional SMC has been employed in [16] to stabilize the translational motion of a quadrotor experimentally.

Generally, sliding motion consists of two phases: reaching phase and sliding phase. In the reaching phase, the system trajectory starts from a given initial condition of the predetermined sliding surface, moves towards it and reaches it in a finite time. In the sliding phase, the motion is restricted to the sliding manifold, lies on it and converges to the desired condition. However, the control system trajectory in the reaching phase is sensitive to external disturbances and uncertainties while the system motion is insensitive against disturbances/parameter variations within sliding phase. There exists a method to enhance the robust performance of the SMC technique by shortening the reaching phase known as Time-Varying Sliding Mode Control (TVSMC). In [17] a stepwise time-varying switching manifold has been introduced. However, this method cannot guarantee insensitivity of the system subject to external disturbances and parameter uncertainties.

In this paper, the problem of attitude control of a 3-DOF quadrotor UAV is investigated experimentally. Accurate quadrotor model is considered such that the centre of mass of the quadrotor does not coincide with the origin of the body-fixed frame. The reminder of this paper is organized as follows: at first, preliminaries for deriving an attitude model of a 3-DOF quadrotor are introduced. Then, a design procedure of an SMC law is developed. Thereafter, numerical simulations and experimental implementations are performed to validate the effectiveness of the designed controller in the presence of the wind gust (as an external disturbance) using an experimental wind tunnel. Finally, this paper is ended with some concluding remarks.

2 Dynamic Model

The dynamical model of a quadrotor consisting of four propellers in cross-shaped frame is studied in this section, as shown in Fig. 1. The attitude change of the quadrotor results from variations on forces and moments produced by adjusting rotors' speeds. To calculate the dynamic model of the quadrotor, the following assumptions have been considered:

- The quadrotor's structure is supposed to be rigid and symmetrical.

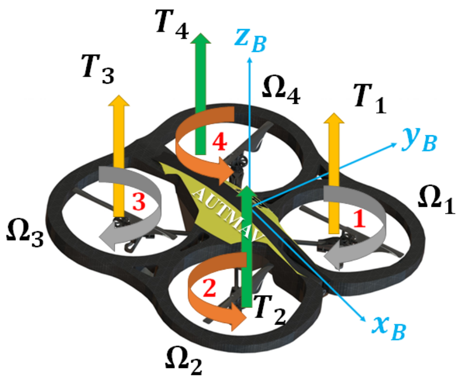

Figure 1: Schematic of the quadrotor configuration with coordinate axes

- The propellers are rigid *i.e.* propeller flapping does not happen.
- The centre of mass does not coincide with the origin of the body-fixed frame.
- Aerodynamic forces and moments are proportional to the square of rotor's speed.
- The axes of the body-frame are coincident with the principle axes of the quadrotor *i.e.* the inertia matrix of the quadrotor is diagonal.

Let $\mathscr{E} = \{x_E, y_E, z_E\}$ be the Earth-fixed inertial frame and $\mathscr{B} = \{x_B, y_B, z_B\}$ denotes the body-fixed frame in which its origin is located in the centre of mass of the quadrotor. The attitude of the quadrotor is described by ZYX Euler angle notations where the Euler angles $\Theta = \begin{bmatrix} \phi & \theta & \psi \end{bmatrix}^T$ are respectively known as roll (rotation around $x-$axis), pitch (rotation around $y-$axis) and yaw (rotation around $z-$axis). Attitude angles are bounded as follows: $\phi \in (-\frac{\pi}{2}, \frac{\pi}{2})$, $\theta \in (-\frac{\pi}{2}, \frac{\pi}{2})$ and $\psi \in (-\pi, \pi)$ because the various acrobatic flying is not admissible. $\omega^B = \begin{bmatrix} p & q & r \end{bmatrix}^T$ represents quadrotor's angular velocity in frame $\mathscr{B}$. The rotational kinematics is obtained from the transformation of the Euler rates $\dot{\Theta} = \begin{bmatrix} \dot{\phi} & \dot{\theta} & \dot{\psi} \end{bmatrix}^T$ measured in the Earth-fixed inertial frame and angular body rates $\omega^B = \begin{bmatrix} p & q & r \end{bmatrix}^T$ as follows:

$$\omega^B = \mathcal{M}\,\dot{\Theta}$$
$$\begin{bmatrix} p \\ q \\ r \end{bmatrix} = \begin{bmatrix} 1 & 0 & -S_\theta \\ 0 & C_\phi & S_\phi C_\theta \\ 0 & -S_\phi & C_\phi C_\theta \end{bmatrix} \begin{bmatrix} \dot{\phi} \\ \dot{\theta} \\ \dot{\psi} \end{bmatrix} \quad (1)$$

where "S" and "C" denote "sin" and "cos" trigonometric functions, respectively. Euler angles are assumed to be small around the hovering position. On the other hand, $\cos\phi = \cos\theta = 1$, $\sin\phi = \phi$ and $\sin\theta = \theta$ are assumed.

The attitude dynamics of the quadrotor can be derived using the Newton-Euler equations in the body frame with the following general formalism:

$$J\dot{\omega}^B + \omega^B \times (J\omega^B) + M_g = \boldsymbol{\tau} \tag{2}$$

where J is an inertia matrix $\Big(J = \mathrm{diag}[J_{xx}, J_{yy}, J_{zz}]\Big)$ of the quadrotor, M_g is the propeller gyroscopic effect and $\boldsymbol{\tau} = \begin{bmatrix} \tau_x & \tau_y & \tau_z \end{bmatrix}^T$ presents the total moments acting on the quadrotor in the body frame. The gyroscopic moment resulting from the propeller's kinetic energies can be described as:

$$M_g = \omega^B \times \begin{bmatrix} 0 & 0 & J_r\Omega_r \end{bmatrix}^T \tag{3}$$

where J_r denotes the propellers' inertia and Ω_r represents the relative propeller's speed which can be defined as:

$$\Omega_r = \sum_{i=1}^{4} (-1)^{i+1}\Omega_i \tag{4}$$

The aerodynamic forces (T) and moments (M) produced by the i^{th} propeller can be expressed as:

$$\begin{aligned} T_i &= k_{Ti}\,{\Omega_i}^2 \\ M_i &= k_{Mi}\,{\Omega_i}^2 \end{aligned} \tag{5}$$

where k_{Ti} and k_{Mi} are aerodynamic constants which can be determined experimentally for each rotor. Then, the total moments $\boldsymbol{\tau}$ can be derived using the following relationship:

$$\begin{cases} \tau_x = \dfrac{\sqrt{2}}{2} L\,(T_1 - T_2 - T_3 + T_4) \\ \tau_y = \dfrac{\sqrt{2}}{2} L\,(-T_1 - T_2 + T_3 + T_4) \\ \tau_z = M_1 - M_2 + M_3 - M_4 \end{cases} \tag{6}$$

where L is a distance between the propeller and the centre of mass of the quadrotor. Hence, control inputs can be described by combining Eqs. (5) and (6) in a vector form as:

$$\begin{bmatrix} u_1 \\ u_2 \\ u_3 \\ u_4 \end{bmatrix} = \begin{bmatrix} 1 & 1 & 1 & 1 \\ \frac{\sqrt{2}}{2}L & -\frac{\sqrt{2}}{2}L & -\frac{\sqrt{2}}{2}L & \frac{\sqrt{2}}{2}L \\ -\frac{\sqrt{2}}{2}L & -\frac{\sqrt{2}}{2}L & \frac{\sqrt{2}}{2}L & \frac{\sqrt{2}}{2}L \\ \frac{k_{M1}}{k_{T1}} & -\frac{k_{M2}}{k_{T2}} & \frac{k_{M3}}{k_{T3}} & -\frac{k_{M4}}{k_{T4}} \end{bmatrix} \begin{bmatrix} T_1 \\ T_2 \\ T_3 \\ T_4 \end{bmatrix} \tag{7}$$

Eventually, the quadrotor attitude dynamics can be written using Eqs. (2) and (7) in the following form:

$$\begin{bmatrix} \ddot{\phi} \\ \ddot{\theta} \\ \ddot{\psi} \end{bmatrix} = \begin{bmatrix} \frac{J_{yy}+mc^2-J_{zz}}{J_{xx}+mc^2}\dot{\theta}\dot{\psi} \\ \frac{J_{zz}-J_{xx}-mc^2}{J_{yy}+mc^2}\dot{\phi}\dot{\psi} \\ \frac{J_{xx}-J_{yy}}{J_{zz}}\dot{\phi}\dot{\theta} \end{bmatrix} - J_r\Omega_r \begin{bmatrix} \frac{\dot{\theta}}{J_{xx}+mc^2} \\ -\frac{\dot{\phi}}{J_{yy}+mc^2} \\ 0 \end{bmatrix} + \begin{bmatrix} \frac{u_2}{J_{xx}+mc^2} \\ \frac{u_3}{J_{yy}+mc^2} \\ \frac{u_4}{J_{zz}} \end{bmatrix} + mgc \begin{bmatrix} -\frac{\sin\phi}{J_{xx}+mc^2} \\ -\frac{\sin\theta}{J_{yy}+mc^2} \\ 0 \end{bmatrix} \tag{8}$$

where c is a distance between the centre of mass and the centre of rotation of the quadrotor. Since propellers are very light, their moment of inertia can be ignored.

3 Controller Design

In this section, sliding mode control (SMC) is designed for stabilization of the attitude of an over-actuated 3-DOF quadrotor.

3.1 Conventional Sliding Mode Control (Conv. SMC)

A conventional sliding surface ($\sigma_{conv.}$) can be expressed as follows:

$$\sigma_{conv.,i} = \dot{\tilde{x}}_i + \lambda_i\,\tilde{x}_i \quad ; \quad i = 1,2,3 \tag{9}$$

where $x_i = \begin{bmatrix} \phi & \theta & \psi \end{bmatrix}^T$ is a state vector, $\tilde{x}$ is a perturbation from the reference ($\tilde{x} = x - x_d$) and λ is a positive constant.

To guarantee the asymptotic stability of the system, consider the following positive-definite function of $\sigma_{conv.}$ as a Lyapunov candidate:

$$V_i = \frac{1}{2}\,{\sigma_{conv.,i}}^2 \tag{10}$$

The time derivative of the Lyapunov candidate can be written in the following form:

$$\begin{aligned} \dot{V}_i &= \sigma_{conv.,i}\,\frac{\partial \sigma_{conv.,i}}{\partial t} \\ &= \sigma_{conv.,i}\,(\ddot{\tilde{x}}_i + \lambda_i\,\dot{\tilde{x}}_i) \end{aligned} \tag{11}$$

According to the Lyapunov's direct method, the negative definiteness of $\dot{V}$ implies that the equilibrium state at the origin is asymptotically stable *i.e.*,

$$\begin{aligned} &\sigma_{conv.,i}\,\frac{\partial \sigma_{conv.,i}}{\partial t} = -\mu_i\,|\sigma_{conv.,i}| \\ \Rightarrow\ &\ddot{\tilde{x}}_i + \lambda_i\,\dot{\tilde{x}}_i = -\mu_i\ \mathrm{sign}\,\sigma_{conv.,i} \end{aligned} \tag{12}$$

where μ is a positive constant. $\mathrm{sign}\,\sigma$ denotes a signum function and can be determined as:

$$\mathrm{sign}\,\sigma = \begin{cases} +1 & \sigma > 0 \\ 0 & \sigma = 0 \\ -1 & \sigma < 0 \end{cases} \tag{13}$$

As a consequence, the nonlinear control inputs are designed using Eqs. (8) and (12) as:

$$\begin{aligned} u_2 =& (J_{xx} + mc^2)\left[\ddot{\phi}_d - \mu_1\,\mathrm{sign}\,\sigma_{conv.,1} - \lambda_1(\dot{\phi} - \dot{\phi}_d)\right] + \\ & (J_{zz} - J_{yy} - mc^2)\,\dot{\theta}\dot{\psi} + J_r\Omega_r\dot{\theta} + mgc\,\sin\phi \end{aligned} \tag{14}$$

,

$$\begin{aligned} u_3 =& (J_{yy} + mc^2)\left[\ddot{\theta}_d - \mu_2\,\mathrm{sign}\,\sigma_{conv.,2} - \lambda_2(\dot{\theta} - \dot{\theta}_d)\right] + \\ & (J_{xx} + mc^2 - J_{zz})\,\dot{\phi}\dot{\psi} - J_r\Omega_r\dot{\phi} + mgc\,\sin\theta \end{aligned} \tag{15}$$

and

$$u_4 = J_{zz}\left[\ddot{\psi}_d - \mu_3 \operatorname{sign}\sigma_{conv.,3} - \lambda_3(\dot{\psi} - \dot{\psi}_d)\right] + (J_{yy} - J_{xx})\,\dot{\phi}\dot{\theta} \tag{16}$$

As it can be seen from Eqs. (13) to (16), signum function is a discontinuous function which can switch the control signal at an infinite frequency and therefore excite the unmodeled fast dynamics or undesired oscillations called *chattering* (or *ripple*). The chattering phenomenon is undesired in practice because it can reduce the system's performance or even lead to instability. Particularly, for a system with flexible appendages, the chattering may disintegrate the whole system. To solve this problem, one may approximate the discontinuous function with a hyperbolic switching function as:

$$u_2 = (J_{xx} + mc^2)\left[\ddot{\phi}_d - \mu_1 \tanh\sigma_{conv.,1} - \lambda_1(\dot{\phi} - \dot{\phi}_d)\right] + (J_{zz} - J_{yy} - mc^2)\,\dot{\theta}\dot{\psi} + J_r\Omega_r\dot{\theta} + mgc\,\sin\phi \tag{17}$$

,

$$u_3 = (J_{yy} + mc^2)\left[\ddot{\theta}_d - \mu_2 \tanh\sigma_{conv.,2} - \lambda_2(\dot{\theta} - \dot{\theta}_d)\right] + (J_{xx} + mc^2 - J_{zz})\,\dot{\phi}\dot{\psi} - J_r\Omega_r\dot{\phi} + mgc\,\sin\theta \tag{18}$$

and

$$u_4 = J_{zz}\left[\ddot{\psi}_d - \mu_3 \tanh\sigma_{conv.,3} - \lambda_3(\dot{\psi} - \dot{\psi}_d)\right] + (J_{yy} - J_{xx})\,\dot{\phi}\dot{\theta} \tag{19}$$

3.2 *Nonsingular Terminal Sliding Mode Control (NTSMC)*

Conventional SMC utilizes a linear switching surface which cannot guarantee the finite time convergence of the state variables. On the other hand, the convergence rate to the desired state variables has an infinite settling time exponentially. In [18], a hierarchical control strategy has been presented theoretically based on the adaptive radical basis function neural networks and an integral SMC for the position and attitude tracking of a quadrotor UAV. Though, the hierarchical control scheme offered fast convergence, it employs larger control domain. To enhance the convergence performance of the traditional sliding mode controller, terminal sliding mode control (TSMC) has been introduced [19]. TSMC uses nonlinear switching manifold in which output errors converge to zero in a finite time. However, TSMC has a critical disadvantage of a singularity problem. Hence, nonsingular terminal sliding mode control (NTSMC) [20] is employed to stabilize the attitude of a quadrotor UAV.

Without loss of generality, a nonsingular terminal sliding manifold can be described as:

$$\sigma_{NTSMC,i} = \tilde{x}_i + \xi_i\,\dot{\tilde{x}}_i^{\frac{\beta_i}{\alpha_i}} \quad ; \quad i = 1,2,3 \tag{20}$$

where α and β are positive odd integers and must satisfy $\alpha < \beta < 2\alpha$. ξ is a positive scalar. The nonlinearity term $\dot{\tilde{x}}_i^{\frac{\beta}{\alpha}}$ in Eq. (20) can improve the convergence speed and assure a bounded control input toward an equilibrium point. To guarantee that the state trajectory remains around the nonsingular terminal switching surface, the following condition should be satisfied:

$$\sigma_{NTSMC,i}\,\frac{\partial\sigma_{NTSMC,i}}{\partial t} < 0 \tag{21}$$

Taking the time-derivative of Eq. (21) along Eq. (20) leads to:

$$\sigma_{NTSMC,i}\,\frac{\partial\sigma_{NTSMC,i}}{\partial t} = \sigma_{NTSMC,i}\Big(\dot{\tilde{x}}_i + \xi_i\frac{\beta_i}{\alpha_i}\,\ddot{\tilde{x}}_i\dot{\tilde{x}}_i^{(\frac{\beta_i}{\alpha_i}-1)}\Big) \tag{22}$$

As a result, to ensure the Lyapunov stability, the following relation should be satisfied:

$$\dot{\tilde{x}}_i^{(2-\frac{\beta_i}{\alpha_i})} + \xi_i\frac{\beta_i}{\alpha_i}\,\ddot{\tilde{x}}_i = -\mu_i\,\operatorname{sign}\sigma_{NTSMC,i} \tag{23}$$

Finally, nonsingular terminal sliding mode controllers can be rewritten as:

$$u_2 = \Big(\ddot{\phi}_d - \mu_1 \operatorname{sign}\sigma_{NTSMC,1} - (\dot{\phi} - \dot{\phi}_d)^{(2-\frac{\beta_1}{\alpha_1})}\Big)(J_{xx} + mc^2)\frac{\alpha_1}{\xi_1\beta_1} + (J_{zz} - J_{yy} - mc^2)\,\dot{\theta}\dot{\psi} + J_r\Omega_r\dot{\theta} + mgc\,\sin\phi \tag{24}$$

,

$$u_3 = \Big(\ddot{\theta}_d - \mu_2 \operatorname{sign}\sigma_{NTSMC,2} - (\dot{\theta} - \dot{\theta}_d)^{(2-\frac{\beta_2}{\alpha_2})}\Big)(J_{yy} + mc^2)\frac{\alpha_2}{\xi_2\beta_2} + (J_{xx} + mc^2 - J_{zz})\,\dot{\phi}\dot{\psi} - J_r\Omega_r\dot{\phi} + mgc\,\sin\theta \tag{25}$$

and

$$u_4 = \Big(\ddot{\psi}_d - \mu_3 \operatorname{sign}\sigma_{NTSMC,3} - (\dot{\psi} - \dot{\psi}_d)^{(2-\frac{\beta_3}{\alpha_3})}\Big)J_{zz}\frac{\alpha_3}{\xi_3\beta_3} + (J_{yy} - J_{xx})\,\dot{\phi}\dot{\theta} \tag{26}$$

As can be observed from Eqs. (24) to (26), nonsingular terminal sliding controllers still include the discontinuous signum function which may cause the chattering phenomenon. To avoid this problem, the signum function can be easily replaced by the hyperbolic function as discussed from Eqs. (14) to (16).

$$u_2 = \Big(\ddot{\phi}_d - \mu_1 \tanh\sigma_{NTSMC,1} - (\dot{\phi} - \dot{\phi}_d)^{(2-\frac{\beta_1}{\alpha_1})}\Big)(J_{xx} + mc^2)\frac{\alpha_1}{\xi_1\beta_1} + (J_{zz} - J_{yy} - mc^2)\,\dot{\theta}\dot{\psi} + J_r\Omega_r\dot{\theta} + mgc\,\sin\phi \tag{27}$$

,

$$\begin{aligned} u_3 =& \Big(\ddot{\theta}_d - \mu_2 \tanh \sigma_{NTSMC,2} - (\dot{\theta} - \dot{\theta}_d)^{(2-\frac{\beta_2}{\alpha_2})}\Big) \\ & (J_{yy} + mc^2)\frac{\alpha_2}{\xi_2 \beta_2} + (J_{xx} + mc^2 - J_{zz})\, \dot{\phi}\dot{\psi} - \\ & J_r \Omega_r \dot{\phi} + mgc\, \sin\theta \end{aligned} \tag{28}$$

and

$$\begin{aligned} u_4 =& \Big(\ddot{\psi}_d - \mu_3 \tanh \sigma_{NTSMC,3} - (\dot{\psi} - \dot{\psi}_d)^{(2-\frac{\beta_3}{\alpha_3})}\Big) \\ & J_{zz}\frac{\alpha_3}{\xi_3 \beta_3} + (J_{yy} - J_{xx})\, \dot{\phi}\dot{\theta} \end{aligned} \tag{29}$$

3.3 Slope-Varying Nonsingular Terminal Sliding Mode Control (SVNTSMC)

In this subsection, a new continuous time-varying switching surface is introduced. The main feature of the proposed time-varying sliding mode control approach is to shorten the reaching phase via continuously rotating switching manifold (known as slope-varying). Therefore, the following sliding manifold is suggested as:

$$\sigma_{SVNTSMC,i} = \tilde{x}_i + f_i(t)\, \xi_i\, \dot{\tilde{x}}_i^{\frac{\beta_i}{\alpha_i}} \quad ; \quad i = 1,2,3 \tag{30}$$

where $f_i(t)$ is a nonlinear time-varying function. It should be noted that the proposed time-varying switching manifold is applicable to any types of SMC approaches, although NTSMC has been chosen because of its aforementioned advantages.

Then, the design procedure of the proposed nonlinear function $f(t)$ is studied. First, the initial values for $f(t)$ function must be described such that the initial states lies on the sliding surface i.e.,

$$f_i(0) = -\frac{\tilde{x}_i(0)}{\xi_i\, \dot{\tilde{x}}_i(0)^{\frac{\beta_i}{\alpha_i}}} \quad ; \quad i = 1,2,3 \tag{31}$$

Thereafter, the function $f(t)$ must be chosen such that the slope-varying sliding manifold approaches the desired sliding surface in a finite time. As an example, one may select the following nonlinear function:

$$f_i(t) = f_i(0) + \Big(1 - f_i(0)\Big) \tanh t \quad ; \quad i = 1,2,3 \tag{32}$$

As a result, slope-varying nonsingular terminal sliding mode controllers can be derived as:

$$\begin{aligned} u_2 =& \Big(\ddot{\phi}_d - \mu_1 \tanh \sigma_{SVNTSMC,1} - (\dot{\phi} - \dot{\phi}_d)^{(2-\frac{\beta_1}{\alpha_1})} - \\ & \xi_1\, \dot{f}_1(t)(\dot{\phi} - \dot{\phi}_d)\Big)(J_{xx} + mc^2)\frac{\alpha_1}{\xi_1 \beta_1\, f_1(t)} + \\ & (J_{zz} - J_{yy} - mc^2)\, \dot{\theta}\dot{\psi} + J_r \Omega_r \dot{\theta} + mgc\, \sin\phi \end{aligned} \tag{33}$$

,

$$\begin{aligned} u_3 =& \Big(\ddot{\theta}_d - \mu_2 \tanh \sigma_{SVNTSMC,2} - (\dot{\theta} - \dot{\theta}_d)^{(2-\frac{\beta_2}{\alpha_2})} - \\ & \xi_2\, \dot{f}_2(t)(\dot{\theta} - \dot{\theta}_d)\Big)(J_{yy} + mc^2)\frac{\alpha_2}{\xi_2 \beta_2\, f_2(t)} + \\ & (J_{xx} + mc^2 - J_{zz})\, \dot{\phi}\dot{\psi} - J_r \Omega_r \dot{\phi} + mgc\, \sin\theta \end{aligned} \tag{34}$$

and

$$\begin{aligned} u_4 =& \Big(\ddot{\psi}_d - \mu_3 \tanh \sigma_{SVNTSMC,3} - (\dot{\psi} - \dot{\psi}_d)^{(2-\frac{\beta_3}{\alpha_3})} - \\ & \xi_3\, \dot{f}_3(t)(\dot{\psi} - \dot{\psi}_d)\Big) J_{zz}\frac{\alpha_3}{\xi_3 \beta_3\, f_3(t)} + (J_{yy} - J_{xx})\, \dot{\phi}\dot{\theta} \end{aligned} \tag{35}$$

To calculate a first component of the control input vector (u_1), let's rewrite T_i from Eq. (7) as:

$$\begin{aligned} T_1 &= \frac{1}{4}u_1 + \frac{\sqrt{2}}{4L}u_2 - \frac{\sqrt{2}}{4L}u_3 + \frac{k_{T1}}{4\, k_{M1}}u_4 \\ T_2 &= \frac{1}{4}u_1 - \frac{\sqrt{2}}{4L}u_2 - \frac{\sqrt{2}}{4L}u_3 - \frac{k_{T2}}{4\, k_{M2}}u_4 \\ T_3 &= \frac{1}{4}u_1 - \frac{\sqrt{2}}{4L}u_2 + \frac{\sqrt{2}}{4L}u_3 + \frac{k_{T3}}{4\, k_{M3}}u_4 \\ T_4 &= \frac{1}{4}u_1 + \frac{\sqrt{2}}{4L}u_2 + \frac{\sqrt{2}}{4L}u_3 - \frac{k_{T4}}{4\, k_{M4}}u_4 \end{aligned} \tag{36}$$

It is apparent from Eq. (36) that each T_i includes a fixed term ($\frac{1}{4}u_1$) and a variable term ($\bar{u}_i$) as:

$$\begin{aligned} \bar{u}_1 &= \frac{\sqrt{2}}{4L}u_2 - \frac{\sqrt{2}}{4L}u_3 + \frac{k_{T1}}{4\, k_{M1}}u_4 \\ \bar{u}_2 &= -\frac{\sqrt{2}}{4L}u_2 - \frac{\sqrt{2}}{4L}u_3 - \frac{k_{T2}}{4\, k_{M2}}u_4 \\ \bar{u}_3 &= -\frac{\sqrt{2}}{4L}u_2 + \frac{\sqrt{2}}{4L}u_3 + \frac{k_{T3}}{4\, k_{M3}}u_4 \\ \bar{u}_4 &= \frac{\sqrt{2}}{4L}u_2 + \frac{\sqrt{2}}{4L}u_3 - \frac{k_{T4}}{4\, k_{M4}}u_4 \end{aligned} \tag{37}$$

Therefore, the minimum value of u_1 can be obtained as:

$$u_1 = 4\, \Big|(\min \bar{u}_i) - T_{min}\Big| \tag{38}$$

where T_{min} is a minimum thrust that can be computed experimentally as $T_{min} = 0.096$ N.

4 Simulation and Experimental Results

This section is dedicated to simulation and real-time experimental validation of the nonsingular terminal sliding mode control (NTSMC) approach for stabilizing the attitude of a 3-DOF quadrotor UAV. The designed experimental test bed is demonstrated in Fig. 2. The quadrotor under investigation consists of an inertial measurement unit (IMU) and an internal computer with a 1 GHz 32 bit ARM Cortex A8 processor. All the measurements collected by the micro-processor with a frequency of 500 Hz is sent to a ground station using a Wi-Fi connection. The testing architecture is developed utilizing a Paparazzi UAV to merge sensors, control law and the communication with the quadrotor. The identified parameters for the experimental test bed are as follows: $m = 0.42$ kg, $L = 0.18$ m, $J_{xx} = J_{yy} = 1.8 \times 10^{-3}$ kg m^2, $J_{zz} = 4.7 \times 10^{-3}$ kg m^2, $J_r = 1.85 \times 10^{-5}$ kg m^2, $k_{Ti} = 5.7 \times 10^{-6}$, $k_{Mi} = 1.7 \times 10^{-7}$, $g = 9.81$ m/s^2 and $c = 3 \times 10^{-2}$ m. In this work, attitude Euler angles are restricted as: $-\frac{\pi}{3} \leq \phi \leq \frac{5\pi}{12}$ and $-\frac{\pi}{3} \leq \theta \leq \frac{\pi}{3}$. Sliding gains are chosen as $\xi_1 = \xi_2 = \xi_3 = 0.5$, $\mu_1 = \mu_2 = \mu_3 = 6$, $\alpha_1 = \alpha_2 = \alpha_3 = 11$ and $\beta_1 = \beta_2 = \beta_3 = 13$.

In this paper, two sliding mode controllers (NTSMC and the proposed SVNTSMC) are applied to a quadrotor subject to the maximum wind velocity (18 m/s). Then, a roll command ($\phi_d = 10$ deg) is executed to the system and attitude stabilization is performed during this maneuver. It is necessary to mention that the wind gust is provided in the AUT wind tunnel, DANA Laboratory.

Attitude tracking of the quadrotor by experiments are shown in Figs. 3 and 4. Fig. 3 displays time history of Euler angles experimentally using NTSMC. Time history of Euler rates are demonstrated in Figs. 5 and 6 based on NTSMC and the proposed SVNTSMC approaches, respectively. From Figs. 3 and 5, one can simply observe that the NTSMC approach is not able to handle large disturbance at the final time. Figs. 4 and 6 prove that the proposed SVNTSMC could successfully enhance the robust tracking performance. In addition, there are some high frequencies present in practice such as unmodeled dynamics, sensor noises and so on that show up in the experimental results.

Figure 2: Experimental test bed of a 3-DOF quadrotor in the AUTMAV laboratory.

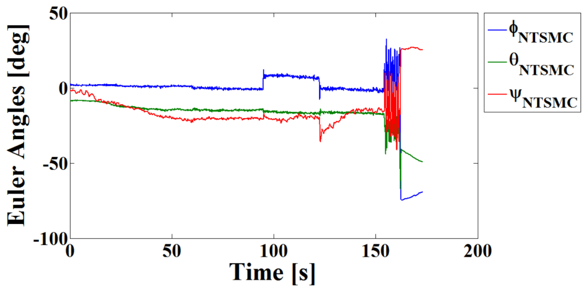

Figure 3: Time history of Euler angles using NTSMC.

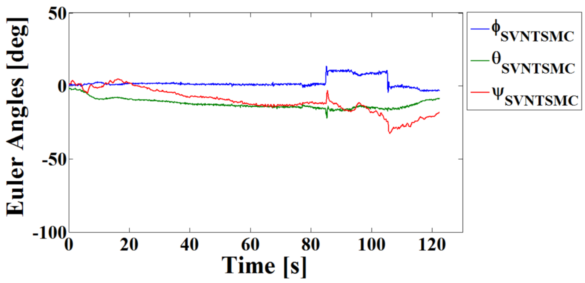

Figure 4: Time history of Euler angles using the proposed SVNTSMC.

5 Conclusion

In this paper, an effective implementation of a nonsingular terminal sliding mode control (NTSMC) approach has been developed for attitude stabilization of a 2-DOF quadrotor. Furthermore, the mathematical model of a quadrotor is derived accurately by considering that the centre of mass of the quadrotor does not coincide with the origin of the body-fixed frame. Traditional sliding mode controllers are not able to tackle any disturbances in the reaching phase. Therefore, a new sliding mode control approach known as Slope-Varying Nonsingular Terminal Sliding Mode Control (SVNTSMC) is proposed to enhance the robust performance of the plant subject to external disturbances. The applied NTSMC and SVNTSMC can assure the finite convergence time of the

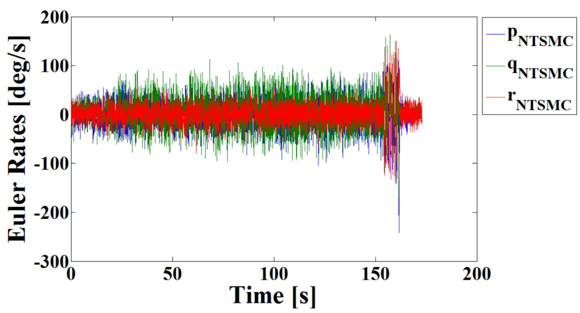

Figure 5: Time history of Euler rates using NTSMC.

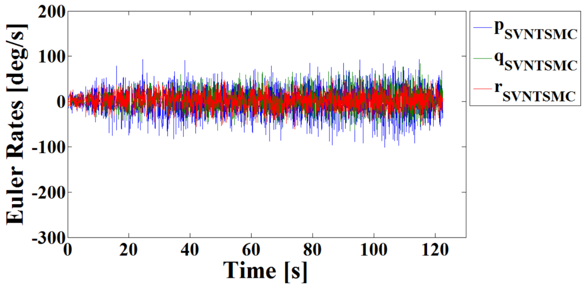

Figure 6: Time history of Euler rates using the proposed SVNTSMC.

state variables as well as singularity avoidance. The chattering phenomenon is eliminated using a smooth approximation of the switching surface around origin. Finally, NTSMC and the proposed SVNTSMC are applied experimentally to a quadrotor subject to a wind gust (as an external disturbance) with high velocity. The comparison between two controllers proved that the proposed SVNTSMC law is effective in practice.

Acknowledgements

This study is supported by National Elites Foundation (known as Bonyad Melli Nokhbegan, BMN, in Persian), Vice-Presidency for Science and Technology, Iran (under grant: 20.152). Authors would like to thank BMN for its support. In addition, gratitude is given to Prof. Mahmoud Mani (Head of Experimental Aerodynamics Research Laboratory known as DANA, Department of Aerospace Engineering, Amirkabir Uniersity of Technology) who graciously allowed us to utilize the wind tunnel setup in the DANA laboratory.

References

[1] J.-J. E. Slotine and W.P. Li. *Applied nonlinear control*. Prentice Hall, Englewood cliffs, 1991.

[2] V.I. Utkin. *Sliding modes in control and optimization*. Springer, New York, NY, 1992.

[3] L. Besnard, Y.B. Shtessel, and B. Landrum. Quadrotor vehicle control via sliding mode controller driven by sliding mode disturbance observer. *Journal of the Franklin Institute*, 349(2):658–684, 2012.

[4] E.-H. Zheng, J.-J. Xiong, and J.-L. Juo. Second order sliding mode control for a quadrotor uav. *ISA Transactions*, 53(4):1350–1356, 2014.

[5] J.-J. Xiong and G.-B. Zhang. Global fast dynamic terminal sliding mode control for a quadrotor uav. *ISA Transactions*, 66:233–240, 2016.

[6] H.J. Jayakrishnan. Position and attitude control of a quadrotor uav using super twisting sliding mode. *IFAC-PapersOnLine*, 49(1):284–289, 2016.

[7] K. Chang, Y. Xia, K. Huang, and D. Ma. Obstacle avoidance and active disturbance rejection control for a quadrotor. *Neurocomputing*, 190:60–69, 2016.

[8] Y. Yang and Y. Yan. Attitude regulation for unmanned quadrotors using adaptive fuzzy gain-scheduling sliding mode control. *Aerospace Science and Technology*, 54:208–217, 2016.

[9] R. Perez-Alcocer, J. Moreno-Valenzuela, and R. Miranda-Colorado. A robust approach for trajectory tracking control of a quadrotor with experimental validation. *ISA Transactions*, 65:262–274, 2016.

[10] D. Cabecinhas, R. Cunha, and C. Silvestre. A nonlinear quadrotor trajectory tracking controller with disturbance rejection. *Control Engineering Practice*, 26:1–10, 2014.

[11] A. Modirrousta and M. Khodabandeh. A novel hybrid controller design for an uncertain quadrotor with disturbances. *Aerospace Science and Technology*, 45:294–308, 2015.

[12] W. Dong, G.-Y. Gu, X. Zhu, and H. Ding. A high-performance flight control approach for quadrotors using a modified active disturbance rejection technique. *Robotics and Autonomous Systems*, 83:177–187, 2016.

[13] F. Munoz, I. Gonzalez-Hernandez, S. Salazar, E.S. Espinoza, and R. Lozano. Second order sliding mode controllers for altitude control of a quadrotor uas: Real-time implementation in quadrotor environments. *Neurocomputing*, 233:61–71, 2016.

[14] A.T. Azar and Q. Zhu. *Advances and applications in sliding mode control systems*. Springer, Switzerland, 2015.

[15] J.A. Moreno. On strict lyapunov functions for some non-homogeneous super-twisting algorithms. *Journal of the Franklin Institute*, 351(4):1902–1919, 2014.

[16] B. Sumantri, N. Uchiyama, and S. Sano. Least square based sliding mode control for a quad-rotor helicopter and energy saving by chattering reduction. *Mechanical Systems and Signal Processing*, 66–67:769–784, 2016.

[17] S.-B. Choi, D.-W. Park, and S. Jayasuriya. A time-varying sliding surface for fast and robust tracking control of second-order uncertain systems. *Automatica*, 30(5):899–904, 1994.

[18] S. Li, Y. Wang, J. Tan, and Y. Zheng. Adaptive rbfnns/integral sliding mode control for a quadrotor aircraft. *Neurocomputing*, 216:126–134, 2016.

[19] S. T. Venkataraman and S. Gulati. Control of nonlinear systems using terminal sliding modes. *Journal of Dynamic Systems, Measurement, and Control*, 115(3):554–560, 1993.

[20] Y. Feng, X. Yu, and Z. Man. Non-singular terminal sliding mode control of rigid manipulators. *Automatica*, 38(12):2159–2167, 2002.